Available online at www.sciencedirect.com

ScienceDirect

Mendeleev Commun., 2022, **32**, 192–193

Mendeleev Communications

DNA penetration into a monolayer of amphiphilic polyelectrolyte

Nikolay S. Chirkov, Alexander V. Michailov, Petr S. Vlasov and Boris A. Noskov*

Institute of Chemistry, St. Petersburg State University, 198504 St. Petersburg, Russian Federation. Fax: +7 812 428 6939; e-mail: b.noskov@spbu.ru

DOI: 10.1016/j.mencom.2022.03.013

Using infrared reflection–absorption spectroscopy, surface tensiometry and atomic force microscopy it is demonstrated that a network of fibrous aggregates of DNA–cationic polyelectrolyte complexes is formed at the water–air interface, the mechanism of the network generation depending on the initial surface pressure of the polyelectrolyte monolayer.

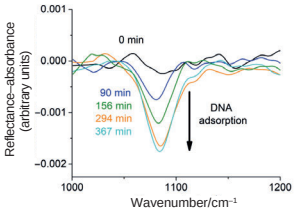

Keywords: DNA, adsorption kinetics, IRRAS, poly[alkyl(diallyl)(methyl)ammonium chloride], Langmuir monolayer, dynamic surface tension.

Mixed solutions of DNA and oppositely charged polyelectrolytes have potential applications in non-viral gene delivery,[1–4] the design of DNA-based chemiresistors[5] and MRI probes.[6] While the properties of DNA–polyelectrolyte complexes in a bulk phase are relatively well investigated, the data on the surface properties of these systems[7,8] are scarce. Two-dimensional structures of DNA can be used as templates for the fabrication of ordered protein nanostructures.[9] However, the formation mechanism for the DNA structures is insufficiently clear, while it is of key importance for the design of films with dedicated properties. It has been shown recently that a network of elongated aggregates is formed at the surface of mixed solutions of DNA with a series of hydrophobic cationic polyelectrolytes.[8] In this work, we investigated the mechanism of the network formation. Poly[diallyl(hexyl)(methyl)-ammonium chloride] (PDAHMAC) as a cationic polyelectrolyte was localized at the buffer–air interface, and the methods of infrared reflection–absorption spectroscopy (IRRAS), surface tensiometry as well as atomic force microscopy (AFM) were applied to trace the changes of surface properties in the course of DNA adsorption.† Note that although IRRAS is occasionally employed to confirm the interaction of DNA with an insoluble monolayer,[10,11] to the best of our knowledge it has never been used to investigate the DNA penetration into a polyelectrolyte monolayer.

IRRAS spectra in general allow separation of signals from different components in the mixed adsorption layer. If the initial surface pressure of the PDAHMAC film is set to 11 mN m^{-1}, only the PDAHMAC band can be seen at ~1255 cm^{-1} [Figure 1(*a*)]. After the DNA injection, two bands emerge at ~1085 and ~1225 cm^{-1} corresponding to the symmetric and asymmetric vibrations of the DNA phosphate groups, respectively.[10] However, their appearance is preceded by a noticeable induction period of ~1.5 h following the DNA injection. After this time, the intensity of the 1085 cm^{-1} band increases abruptly, reaching an almost constant value in ~5 h post injection [Figure 1(*b*)]. If the initial surface pressure of the PDAHMAC film is set to 7 mN m^{-1}, the corresponding changes in the IRRAS bands agree qualitatively with the former case, though the induction period is shorter and the intensity of the 1085 cm^{-1} band starts to increase in ~1 h after the injection of DNA, reaching a constant value in ~4 h [Figure 2(*a*),(*b*)].

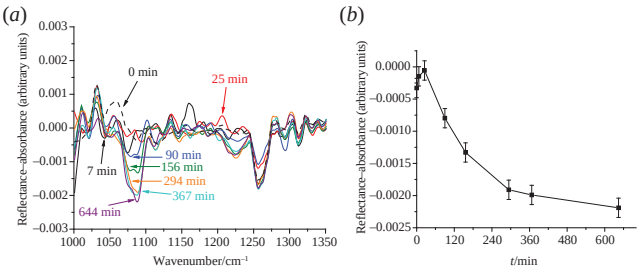

Figure 1 (*a*) IRRAS spectra of a PDAHMAC layer before (dashed black line) and at different time after DNA injection into the subphase. (*b*) Reflectance–absorbance of the 1085 cm^{-1} band *vs.* time after the injection. Total DNA concentration is 56 μmol dm^{-3}, initial surface pressure of the PDAHMAC monolayer is 11 mN m^{-1}.

† PDAHMAC was synthesized by the radical polymerization of diallyl(hexyl)(methyl)ammonium chloride as described.[12] Sodium chloride (Vekton, Russia) was calcinated in a muffle furnace for 6 h at ~800 °C to eliminate organic impurities. All the solutions were prepared in triply distilled water. Calf thymus DNA fibers (Sigma-Aldrich) were dissolved in 10 mM Tris–HCl buffer solution (from Trizma base, Sigma-Aldrich) containing 20 mM NaCl, pH 7.6. The stock DNA solution was stored at 4 °C for no longer than 2 weeks. PDAHMAC solution (70 and 40 μl, 0.2 g dm^{-3}) in MeOH (Vekton, Russia) was spread onto the surface of the buffer solution with a surface area of 6.8 × 10^{-3} m^2 to attain two different surface pressure values (11 and 7 mN m^{-1}, respectively). Then an appropriate amount of the DNA stock solution was injected into the subphase by a glass syringe. The surface tension data were collected using the Wilhelmy plate method with a sandblasted glass plate attached to an electronic balance,[13] IRRAS spectra employing a Nicolet 8700 FTIR spectrometer (Thermo Fisher Scientific, USA) equipped with a Tabletop Optical Module (TOM)[14] were obtained as described.[13] The compression isotherm was recorded on a KSV NIMA instrument (KSV Instruments, Finland). The mixed films of DNA and PDAHMAC were transferred from the liquid surface onto a freshly cleaved mica plate by the Langmuir−Schaefer technique,[15] dried for at least 3 days in a desiccator at 4 °C and then investigated by AFM using an NTEGRA Prima setup (NT-MDT, Russia). All the measurements were carried out at 20 ± 1 °C.

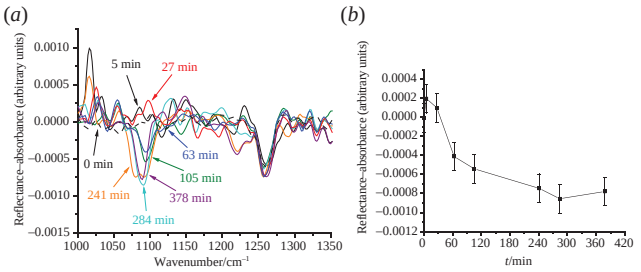

Figure 2 (*a*) IRRAS spectra of a PDAHMAC layer before (dashed black line) and at different time after DNA injection into the subphase. (*b*) Reflectance–absorbance of the 1085 cm^{-1} band *vs.* time after the injection. Total DNA concentration is 56 μmol dm^{-3}, initial surface pressure of the PDAHMAC monolayer is 7 mN m^{-1}.

Although the IRRAS signal increases uniformly after the DNA injection, the corresponding changes of surface pressure are non-monotonic [Figure 3(*a*)]. If the initial value of the surface pressure is set to 11 mN m^{-1}, it starts to decrease after a long induction period, reaching a minimum value of 5 mN m^{-1} in ~13 h. After that, it slightly increases to 6 mN m^{-1}. Different induction periods in the spectroscopic and tensiometric experiments can be attributed to a distinct size of the measurement cells, which influence the self-convection and, therefore, the adsorption kinetics. Note that a decrease in surface pressure upon DNA addition into the subphase has been observed for cationic lipid monolayers.[16] It is known, that the formation of DNA–polyelectrolyte complexes represents a spontaneous process, the main driving force being the entropy gain as a result of a counterion release.[17] When such a process occurs in the surface layer, it leads to transition of some polyelectrolyte segments from proximal region of the surface layer into the distal one, thus lowering the surface pressure. Besides, since the absorption length of IR radiation in this spectral range is a few orders of magnitude larger than the PDAHMAC film thickness, such a transition does not induce a decrease in the intensity of the polymer band in the IRRAS spectrum (see Figures 1 and 2). The desorbed polyelectrolyte segments do not dissolve into the bulk and remain in the vicinity to the surface, keeping the IRRAS signal constant while lowering the surface pressure. A part of the desorbed segments eventually readsorbs and thus increases the surface pressure after attaining the minimum value. The last step of the mixed layer formation consists in the emergence of a network of interlinked DNA–PDAHMAC fibrous aggregates, similar to those found in mixed adsorption layers[8] [see Figure 3(*a*), inset].

If the initial surface pressure is set to 7 mN m^{-1}, the corresponding changes in both the IRRAS spectra and the surface pressure data occur much faster. The minimum of surface pressure is recorded in ~2 h after the DNA injection and the surface pressure changes only slightly at the approach to equilibrium after a relatively fast increase beyond the local minimum. Note that the final value of the surface pressure matches the initial one, namely

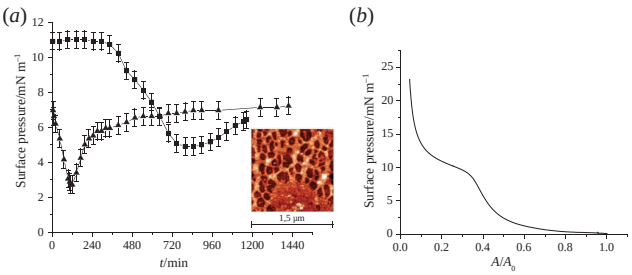

Figure 3 (*a*) Surface pressure of a PDAHMAC layer *vs.* time after DNA injection into the subphase. Total DNA concentration is 56 μmol dm^{-3}, the initial surface pressure of the PDAHMAC monolayer is (■) 11 mN m^{-1} and (▲) 7 mN m^{-1}. Inset: AFM image of the spread PDAHMAC layer transferred onto a mica surface at 1200 min after DNA injection into the subphase, the initial surface pressure of the layer is 11 mN m^{-1}. (*b*) Surface pressure *vs.* relative surface area for a PDAHMAC layer spread onto buffer solution.

7 mN m^{-1}, unlike the case of higher initial surface pressure. This is probably due to the larger surface concentration of PDAHMAC at 11 mN m^{-1}, which hinders the readsorption of the DNA–PDAHMAC complexes. An increase in the adsorption rate with a decrease in the initial surface pressure can be explained from the PDAHMAC compression isotherm [Figure 3(*b*)] as a plot of surface pressure *vs.* relative surface area A/A_0, where A_0 is the initial surface area of the Langmuir trough. A quasiplateau presumably connected with a two-dimensional phase transition can be seen at surface pressures close to 11 mN m^{-1}. Here the PDAHMAC layer is close-packed and creates steric hindrance for the negatively charged phosphate groups of DNA to approach a positively charged nitrogen atom of PDAHMAC. When the initial surface pressure is lowered to 7 mN m^{-1}, the PDAHMAC layer becomes more fluid-like, the energetic barrier for the complex formation decreases and the rate of DNA–polyelectrolyte interactions increases strongly leading to a substantial lowering of the induction period of both the IRRAS intensity and the time dependence of surface pressure. The obtained results reveal that the formation of a network of threadlike DNA–PDAHMAC aggregates occurs at the interface or in its close vicinity, *i.e.*, in the regions of high local concentration of the components. This scenario of the network formation can be applied to the mixed DNA–PDAHMAC solutions.[8]

This work was supported by the Russian Science Foundation (project no. 21-13-00039). The authors are also grateful to the resource centers of St. Petersburg State University, namely the Centre for Optical and Laser Materials Research, the Chemical Analysis and Materials Research Centre, the Centre for Diagnostics of Functional Materials for Medicine, Pharmacology and Nanoelectronics as well as the Interdisciplinary Resource Centre for Nanotechnology, for the use of their equipment.

References

1 S. Sakai, Y. Yamada, T. Yamaguchi, T. Ciach and K. Kawakami, *J. Biomed. Mater. Res., Part A*, 2009, **88**, 281.
2 Y. Yang, X. Li, L. Cheng, S. He, J. Zou, F. Chen and Z. Zhang, *Acta Biomater.*, 2011, **7**, 2533.
3 D. Fischer, H. Dautzenberg, K. Kunath and T. Kissel, *Int. J. Pharm.*, 2004, **280**, 253.
4 M. Alatorre-Meda, P. Taboada, B. Krajewska, M. Willemeit, A. Deml, R. Klösel and J. R. Rodríguez, *J. Phys. Chem. B*, 2010, **114**, 9356.
5 W. Wang, K. Zhang and D. Chen, *Langmuir*, 2018, **34**, 15350.
6 Y. Zou, Y. Li, J. Xu, X. Huang and D. Chen, *Polym. Chem.*, 2020, **11**, 6134.
7 P.-W. Yang, T.-L. Lin, I-T. Liu, Y. Hu and M. James, *Soft Matter*, 2012, **8**, 7161.
8 N. S. Chirkov, A. V. Akentiev, R. A. Campbell, S.-Y. Lin, K. A. Timoshen, P. S. Vlasov and B. A. Noskov, *Langmuir*, 2019, **35**, 13967.
9 P. L. Xavier and A. R. Chandrasekaran, *Nanotechnology*, 2018, **29**, 062001.
10 S. Gromelski and G. Brezesinski, *Langmuir*, 2006, **22**, 6293.
11 Q. Chen, X. Kang, R. Li, X. Du, Y. Shang, H. Liu and Y. Hu, *Langmuir*, 2012, **28**, 3429.
12 N. V. Tsvetkov, A. A. Lezov, P. S. Vlasov, A. A. Lezova, S. A. Samokhvalova, E. V. Lebedeva and G. E. Polushina, *Eur. Polym. J.*, 2016, **84**, 268.
13 V. V. Lyadinskaya, S.-Y. Lin, A. V. Michailov, A. V. Povolotskiy and B. A. Noskov, *Langmuir*, 2016, **32**, 13435.
14 A. Michailov, A. Povolotskiy and V. Kuzmin, *Opt. Express*, 2021, **29**, 3090.
15 I. Langmuir and V. J. Schaefer, *J. Am. Chem. Soc.*, 1938, **60**, 1351.
16 C. Janich, A. Hädicke, U. Bakowsky, G. Brezesinski and C. Wölk, *Langmuir*, 2017, **33**, 10172.
17 M. Buriuli and D. Verma, in *Advances in Biomaterials for Biomedical Applicationss*, eds. A. Tripathi and J. S. Melo (*Advanced Structural Materials*, vol. 66), Springer, Singapore, 2017, pp. 45–93.

Received: 22nd July 2021; Com. 21/6621